4

DTIC FILE COPY

GL-TR-89-0221

AD-A219 549

SH Wave Scattering From a Sinusoidal Grating

H. D. Axilrod
J. F. Ferguson

Center for Lithospheric Studies
The University of Texas at Dallas
P. O. Box 830688
Richardson, TX 75083-0688

1 August 1989

Final Report
March 1987-March 1989

APPROVED FOR PUBLIC RELEASE; DISTRIBUTION UNLIMITED

GEOPHYSICS LABORATORY
AIR FORCE SYSTEMS COMMAND
UNITED STATES AIR FORCE
HANSCOM AIR FORCE BASE, MASSACHUSETTS 01731-5000

SPONSORED BY
Defense Advanced Research Projects Agency
Nuclear Monitoring Research Office
ARPA ORDER NO. 5299

MONITORED BY
Geophysics Laboratory
Contract No. F19628-87-K-0029

The views and conclusions contained in this document are those of the authors and should not be interpreted as representing the official policies, either expressed or implied, of the Defense Advanced Research Projects Agency or the U.S. Government.

This technical report has been reviewed and is approved for publication.

JAMES F. LEWKOWICZ
Contract Manager
Solid Earth Geophysics Branch
Earth Sciences Division

JAMES F. LEWKOWICZ
Branch Chief
Solid Earth Geophysics Branch
Earth Sciences Division

FOR THE COMMANDER

DONALD H. ECKHARDT, Director
Earth Sciences Division

This report has been reviewed by the ESD Public Affairs Office (PA) and is releasable to the National Technical Information Service (NTIS).

Qualified requestors may obtain additional copies from the Defense Technical Information Center. All others should apply to the National Technical Information Service.

If your address has changed, or if you wish to be removed from the mailing list, or if the addressee is no longer employed by your organization, please notify AFGL/DAA, Hanscom AFB, MA 01731-5000. This will assist us in maintaining a current mailing list.

Do not return copies of this report unless contractual obligations or notices on a specific document requires that it be returned.

Unclassified
SECURITY CLASSIFICATION OF THIS PAGE

REPORT DOCUMENTATION PAGE

Form Approved
OMB No. 0704-0188

1a. REPORT SECURITY CLASSIFICATION Unclassified	1b RESTRICTIVE MARKINGS
2a. SECURITY CLASSIFICATION AUTHORITY	3. DISTRIBUTION/AVAILABILITY OF REPORT Approved for Public Release Distribution unlimited
2b. DECLASSIFICATION/DOWNGRADING SCHEDULE	
4. PERFORMING ORGANIZATION REPORT NUMBER(S)	5. MONITORING ORGANIZATION REPORT NUMBER(S) GL-TR-89-0221
6a. NAME OF PERFORMING ORGANIZATION University of Texas at Dallas 6b. OFFICE SYMBOL (If applicable)	7a. NAME OF MONITORING ORGANIZATION Geophysics Laboratory
6c. ADDRESS (City, State, and ZIP Code) P.O. Box 830688 Richardson, TX 75083-0688	7b. ADDRESS (City, State, and ZIP Code) Hanscom AFB, MA 01731-5000
8a. NAME OF FUNDING/SPONSORING ORGANIZATION Defense Advanced Research Projects Agency 8b. OFFICE SYMBOL (If applicable) NMRO	9 PROCUREMENT INSTRUMENT IDENTIFICATION NUMBER F19628-87-K-0029
8c. ADDRESS (City, State, and ZIP Code) 1400 Wilson Blvd. Arlington, VA 22209-2308	10. SOURCE OF FUNDING NUMBERS PROGRAM ELEMENT NO. 61101E; PROJECT NO. 7410; TASK NO DA; WORK UNIT ACCESSION NO. CV

11. TITLE (Include Security Classification)
SH Wave Scattering From a Sinusoidal Grating

12. PERSONAL AUTHOR(S)
H. D. Axilrod and J. F. Ferguson

13a. TYPE OF REPORT	13b. TIME COVERED	14. DATE OF REPORT (Year, Month, Day)	15. PAGE COUNT
Final Report	FROM 3/87 TO 3/89	1989, August, 1	46

16. SUPPLEMENTARY NOTATION

17. COSATI CODES			18. SUBJECT TERMS (Continue on reverse if necessary and identify by block number)
FIELD	GROUP	SUB-GROUP	Seismic modeling, non-horizontal layering, scattering numerical modeling

19. ABSTRACT (Continue on reverse if necessary and identify by block number)

A good way to test discrete wavenumber modeling techniques is to model scattering from a sinusoidal free surface, while varying the maximum slope of the interface. Four discrete wavenumber methods, the Aki-Larner, the Waterman, the Waterman-Fourier, and the Campillo-Bouchon, are evaluated by testing for energy conservation and comparing displacement. Contrary to the claim of some authors (Varadan et al. 1987), the Waterman-Fourier shows no advantage over the Aki-Larner method for steep slopes. With the novel use of an FFT to calculate the scattering matrix, the Waterman-Fourier method is as fast as Aki-Larner. The Campilio-Bouchon method is superior to the other methods in its ability to handle steep slopes, but it requires more wavenumber samples and is an order of magnitude slower.

20 DISTRIBUTION/AVAILABILITY OF ABSTRACT ☐ UNCLASSIFIED/UNLIMITED ☐ SAME AS RPT. ☐ DTIC USERS	21. ABSTRACT SECURITY CLASSIFICATION Unclassified
22a NAME OF RESPONSIBLE INDIVIDUAL James F. Lewkowitz	22b. TELEPHONE (Include Area Code) (617) 377-3222 22c. OFFICE SYMBOL GL/LWH

DD Form 1473, JUN 86 — Previous editions are obsolete. — SECURITY CLASSIFICATION OF THIS PAGE

Unclassified

INTRODUCTION

Wave scattering from a sinusoidal grating has been a problem of considerable interest in a number of disciplines. It is of interest in seismology for modeling the affects of topography on seismic wave propagation. Many of the discrete wavenumber modeling techniques that have been developed for sinusoidal gratings are also applicable to interfaces of arbitrary shape.

In this paper we will compare results and numerical properties of four different discrete wavenumber modeling techniques. All of the comparisons are done for the simple problem of a sinusoidal free surface grating with a vertically traveling plane wave incident from below (Figure 1). Particle motion is parallel to the strike of the structure (SH waves). The modeling methods we will examine are the Aki-Larner method (1970), the Waterman method (1975), the Waterman-Fourier method (Varaden, et al. 1987), and the Campillo-Bouchon method (1987). We will refer to these methods as AL, WR, WF, and CB, respectively. All of these techniques are applicable to interfaces of arbitrary shape and can in principle be generalized, to fully elastic, multi-layer, and 3-D models.

A solution to the sinusoidal grating problem was proposed by Rayleigh (1907). He expanded the wavefield in terms of up and down going plane waves and solved for the coefficients by satisfying the stress free boundary condition at a number of points along the surface. AL is essentially an overdetermined, least squares version of the Rayleigh method, formulated in the wavenumber domain. However, since Lippmann (1953) questioned the expansion used in the Rayleigh method, the so called "Rayleigh *ansatz*", the history of this modeling approach has been shrouded in controversy. Lippmann suggested that the Rayleigh expansion is satisfactory below a plane bounding the topography, but is unsatisfactory inside the the peaks (Figure 2).

Petit and Cadilhac (1966) proved that the Rayleigh *ansatz* could not be valid if the ratio of the amplitude to the wavelength of the sinusoid (h/L) is greater than 0.072. Millar (1971) proved that the Rayleigh *ansatz* is in fact valid if h/L is less than 0.072. Other authors have shown, e.g. Wirgin (1980) and Jiracek (1973), that the Rayleigh *ansatz* is usable for slopes greater than the Millar limit. There continues to be heated debate over this issue. (See Wirgin 1986, and Lakhtakia et al., 1986.)

In addition to the controversy over the validity of the Rayleigh *ansatz*, there has been discussion as to whether the Waterman method (WR) uses the *ansatz*. Basically this method, also known as the T-matrix method, makes use of the Helmholtz formula to generalize the boundary conditions. Waterman originally claimed that his approach was not dependent on the *ansatz*. Today, it is generally accepted that WR uses the *ansatz* and is therefore limited by the slope of the interface (Lakhtakia et al., 1985b).

WF is an alternative formulation of the Waterman method that uses the expansion proposed by Masel et al. (1975) instead of the Rayleigh *ansatz*. In principle, it is not limited by the slope of the interface.

The Campillo and Bouchon method (CB) resembles the aforementioned techniques in some ways, and it is clearly independent of the Rayleigh ansatz. CB is a collocation method similar to AL, but it parameterizes the reflected wavefield in terms of line (or point) sources distributed along the interface.

We will compare and evaluate the four techniques as they apply to the sinusoidal free surface, SH wave problem. In particular we will map the region of energy conservation with respect to slope (h/L), frequency (k·L), and N (the number of plane waves used in the expansion). We will also examine the wavefield, at the interface and below the lower bounding plane of the topography.

METHODS

In this section a unified description of the four methods will be given in order to define the common features. All of them operate on time harmonic solutions to the wavefields, and the time dependence, $\exp(i\omega t)$, is suppressed. In all four methods the model is assumed to be periodic in the x-direction, leading to a discrete plane wave representation of the wavefield. The x and z wavenumber components are:

$$k_n = 2\pi n/L \tag{1}$$

and

$$\gamma_n = (\omega^2/\beta^2 - k_n{}^2)^{1/2} \tag{2}$$

where

$$\beta = (\mu/\rho)^{1/2} = \text{shear wave velocity.} \tag{3}$$

Effects of adjacent periods can be suppressed by adding a small imaginary component to ω which can be defined in terms of a realistic Q parameter. Each of the methods can be stated in matrix form.

For AL, the matrix representation is,

$$\mathbf{a} = \mathbf{G}\,\mathbf{r} \tag{4}$$

where

r_n = the coefficients in the Rayleigh expansion for the reflected waves, i.e.,

$$U_R = \sum_{-\infty}^{\infty} r_n\, e^{i(k_n x + \gamma_n z)} \qquad z \geq \xi(x) \tag{5}$$

a_m = the Fourier transform of the traction on the interface surface due to the incident field. For a vertically traveling plane wave of unit amplitude,

$$a_m = i\mu\gamma_0/L \int_0^L n_z \, e^{i\gamma_0 \xi(x)} \, e^{-k_m x} \, dx. \tag{6}$$

And

$$G_{mn} = -i\mu/L \int_0^L \hat{n} \cdot k \, e^{i(k_n - k_m)x} \, e^{i\gamma_n \xi(x)} \, dx. \tag{7}$$

Truncation of the series (5) and discretization of integrals (6) and (7) leads to a least squares solution,

$$\left.\begin{matrix} n \\ m \end{matrix}\right\} = -M, \cdot \cdot \cdot, 0, \cdot \cdot \cdot, +M \tag{8}$$

where

$$N = 2M + 1. \tag{9}$$

The solution to (4) minimizes the normal stress at the surface sample points in a least squares sense. The vector **a** and columns of the matrix **G** can be calculated using the fast Fourier transform (FFT). In this study we use an FFT of length 128 and solve for a vector **r** of length N. With N < 128, the problem is overdetermined.

The Waterman method derives from the Helmholtz formula equations (10 and 11), after plane wave expansions have been substituted for the Green's functions and the wavefields.

Equation 10 represents Huygen's principle, and equation 11 is the extended boundary condition. (Waterman 1975)

$$\left.\begin{array}{l} U_R(z \geq \xi) \\ U_I(z < \xi) \end{array}\right\} = 1/4i \int_{-\infty}^{+\infty} \hat{\mathbf{n}} \cdot [U^+ \nabla g - g \nabla U^+] \, dx \qquad \begin{array}{r} (10) \\ (11) \end{array}$$

where

g = the free space Green's function,

and

U^+ = the wavefield on the interface.

Note that $\hat{\mathbf{n}} \cdot \nabla U^+ = 0$ on a free surface.

Modeling using WR or WF requires that we solve the following coupled set of matrix equations.

$$\mathbf{r} = \mathbf{Q}^+ \boldsymbol{\alpha} \tag{12}$$

$$\mathbf{b} = \mathbf{Q}^- \boldsymbol{\alpha} \tag{13}$$

where

r_n = the coefficients of the reflected wavefield as in AL, except the domain is limited to $z > h$,

b_n = the coefficients of the incident wavefield, i.e.,

$$b_n = \begin{cases} 1 & n = 0 \\ 0 & n \neq 0 \end{cases} \tag{14}$$

and

α_m = the coefficients of the surface field expansion.

For WR,

$$U^+ = \sum_{m=-M}^{+M} \alpha_m \, e^{i(k_m x - \gamma_m \xi(x))} \tag{15}$$

$$Q^{\pm}_{nm} = i/kL \int_0^L (\gamma_m - k_m n_x/n_z)\, e^{i(k_m x \pm \gamma_n \eta)}\, e^{i(k_n x - \gamma_m \xi)}\, dx \qquad (16)$$

and for WF,

$$U^{+} = \sum_{m=-M}^{+M} \alpha_m\, e^{ik_m x} \qquad (17)$$

$$Q^{\pm}_{nm} = i/kL \int_0^L (\gamma_m - k_m n_x/n_z)\, e^{i(k_m x \pm \gamma_n \xi)}\, e^{ik_n x}\, dx \qquad (18)$$

Equations 12 and 13 correspond to equations 16 and 18, respectively, with an implied trucation length of 2M+1 wavenumber samples. Equation 15 is equivalent to the Rayleigh *ansatz* expansion, albeit expressed in terms of upgoing instead of downgoing waves. If we use the alternative surface field expansion proposed by Masel et al. (1975), the matrix equations represent the Waterman Fourier method (WF).

It is interesting to note that although they are used in a completely different context, the $\mathbf{Q}^{-}$ matrix for WF is nearly identical to the transpose of the $\mathbf{G}$ matrix used in AL. The two integral expression are the same except for a factor (n_z) in the integrand. This suggests that the elements of the $\mathbf{Q}$ matrix can be generated a row at a time using an FFT. For a sinusoidal interface, the integral (18) simplifies to a Bessel function. However, in this study we will calculate the $\mathbf{Q}$ matrices using FFT's, as we would for an interface of arbitrary shape. A sample length of 128 is used, the same as with AL.

A normalization scheme can be applied to WR or WF to improve stability. The details of this scheme are in Appendix I.

The CB method is a collocation method like AL. Unlike the other methods, however, the coefficient vector is in the space domain rather than the horizontal wavenumber domain. The wavefield is expanded in a series of line sources equally distributed in x along the interface:

$$x_n = (n-1)\ L/N. \tag{19}$$

For CB the matrix representation is

$$\mathbf{c} = \mathbf{B}\ \mathbf{f} \tag{20}$$

where

c_n = the traction on the interface due to the incident field, i.e.,

$$c_n = i\ \mu\ n_z\ \gamma_o\ e^{i\gamma_o \xi(x_n)} \tag{21}$$

f_m = the line source coefficients, i.e.,

$$U_R = 1/(2i\mu L) \sum_{m=-M}^{+M} f_m \sum_{p=-M}^{+M} (1/\gamma_p)\ e^{i\gamma_p |z - \xi_m|}\ e^{ik_p(x - x_m)} \tag{22}$$

and

$$B_{nm} = 1/(2i\mu) \sum_{p=-M}^{+M} (i\hat{n}\cdot k/\gamma_p)\, e^{i\gamma_p |z_n - \zeta_m|}\, e^{ik_p(x_n - x_m)} \tag{23}$$

The use of the line source expansion (22) replaces the Rayleigh *ansatz* and Masel expansions used in [illegible] and WF, respectively. Equation (20) extinguishes the normal stress at the source points; it is even-determined, with as many equations as there are line sources. We could formulate CB using an overdetermined least squares solution at the cost of an additional loop in the calculation of the matrix elements. This addition would be costly in terms of execution time.

RESULTS

A simple way to evaluate the four techniques is to test for energy conservation. In each numerical experiment we assume that a monocromatic, vertically traveling plane wave of unit amplitude is incident on a sinusoidal free surface. Energy conservation requires that the reflected energy flux equals the incident energy flux, i.e.,

$$\sum_{n=-M}^{+M} |r_n|^2 \frac{\mathrm{Re}(\gamma_n)}{|\gamma_n|} = 1, \tag{24}$$

as used by others (Larner 1970, Lakhtakia et al. 1985a).

The interface slope is described by h/L, the ratio of the amplitude to the period of the sinusoid. The frequency of the incoming energy is described by k·L, the normalized frequency. It is also necessary to specify N, the number of coefficients or discrete wavenumbers samples to be used in a particular numerical experiment. The region of energy conservation in the two dimensional {N-(k·L)} domain has been mapped for each of the modeling techniques and for various interface slopes.

A number of features in the energy conservation maps are worthy of mention. As the normalized frequency increases, more coefficients are needed to obtain convergence and energy conservation. This is expected because with increasing frequency more of the coefficients represent propagating waves. The WR, WF, and AL techniques are all limited to a maximum wavenumber beyond which the solution diverges and energy is not conserved. CB does not appear to have such a limit.

For the methods that are wavenumber limited, the maximum number of samples, N_{max}, depends on frequency and h/L, the slope of the interface. For steep slopes ($h/L \geq 0.15$) there is an upper limit on the frequency for which convergence occurs at any wavenumber. Therefore, when we discuss slope limitations for a particular modeling method we must also specify frequency.

Note that the wavenumber limit is a numerical feature not necessarily related to the Rayleigh *ansatz*. For example, the WF method which does not invoke the Rayleigh *ansatz* has an N_{max} for slopes both above and below the Millar limit of $h/L = 0.072$. Also the the WR and AL methods have wavenumber limits for h/L less than 0.072.

Further scrutiny of Figure 3 reveals that N_{max} is always in the evanescent wave region where coefficient amplitudes increase exponentially with z. Use of these waves in the solution will eventually exceed the precision and wordsize of the computer. The convergence range can of course be extended by increasing the word length and precision.

The most significant feature of the energy conservation maps is that the WF and AL methods have very similar regions of convergence. For steep slopes, the two methods show convergence up to about the same maximum frequency. For h/L = 0.1, AL and WF are nearly the same except WF diverges somewhat more rapidly as N increases. For h/L = 0.072, there is a more dramatic difference in the rate of divergence. Nonetheless, these data support the observation made by Wirgin (1980), that regardless of the Rayleigh *ansatz*, the WF and AL methods are limited to the same maximum slope.

The performance of WR falls short of WF or AL. For gradual slopes, WR has lower N_{max} values, and for steep slopes WR does not converge at all. It is no surprise that WR would have a lower N_{max} than WF since Waterman's original surface field expansion introduces an additional exponential factor in the calculation of the Q-matrix elements. (Equation 15 as compared to equation 17.)

Use of the normalization technique described in Appendix I alters the region of convergence for the WR and WF methods. The normalization does not extend the maximum allowable slope, but it does increase N_{max}, allowing more coefficients to be used, especially at frequencies below the maximum for a particular slope. With the normalization, the region of energy conservation for the WF method and the AL method are nearly identical even at low slopes (Figure 4). The region of convergence for the WR method is also extended by use of the normalization.

The convergence characteristics of the CB method are substantially different from the other three methods. For CB there is apparently no limit due to the exponential factors associated with evanescent waves. The absolute value in the formulation of the CB method ensures that only exponentially decaying factors are in the matrix elements. In general, more wavenumber samples are needed with the CB method to obtain the same accuracy in energy conservation as with the other methods. This may be partially due to the fact that CB is an even-determined collocation method as opposed to AL which is over-determined.

The conservation of energy constraint is one way to evaluate the four modeling techniques. Another such test is the satisfaction of boundary conditions. Unfortunately, for some of the techniques this is neither practical nor possible. As formulated, the CB method is even-determined and the residuals of normal stress are always zero. For the Waterman techniques there is no valid expression for the stress at the interface. The expansion of the Green's function in terms of only upgoing or downgoing waves, yields a reflected wavefield solution that is valid only in the region below the lower bounding plane.

An alternative evaluation for the modeling techniques is to compare the displacements at the interface. It is possible to calculate displacements at the interface with all of the methods, even the Waterman techniques because equations 15 and 17 do apply immediately at the surface.

Although there is no boundary condition for displacements to satisfy, they can be used to test for consistency between the methods. Figure 5 shows surface displacements calculated with each of the modeling techniques for interfaces of low, moderate, and steep slope. In each case an appropriate frequency and number of samples have been chosen, i.e., well within the region of energy conservation.

For small slopes, ($h/L = 0.1$) all four methods agree well in terms of surface displacement. Note that the AL and WR methods agree with the others despite the fact that the slope is beyond Millar's theoretical Rayleigh limit of 0.072.

For the medium and steep slope models, the results are different. We see that the WF and CB methods agree well in terms of displacement on the surface, but WR and AL show marked differences. WR does not satisfy the energy conservation constraint for these parameters, so it is not surprising that the surface displacements are different. For AL the energy conservation constaint is satisfied, but the method fails to yield correct surface displacements for slopes significantly beyond the Rayleigh limit.

It is useful to compare the wavefields not only at the surface, but also below the lower bounding plane of the topography. One way to do this is to look at displacements at the lower bounding plane ($z = h$). Another way is to compare the amplitude spectra of the reflected energy. Figure 6 shows the displacements at $z = h$ for the same slope and frequency cases for which we examined surface displacements. For $h/L = 0.1$ all four methods agree closely. For the steeper slope, WF, AL and CB agree, but WR fails to give a consistent result. The amplitude spectra in Figure 7 show the same pattern of consistency. For steep slope the spectrum for WR blows up in the evanescent wavenumber range, but the other methods agree reasonably well. (Note the logarithmic scale.)

For slope greater than the Millar limit AL fails to yield surface displacements consistent with the other methods, but it appears to give the correct result below the lower bounding plane.

COMPUTATIONAL CONSIDERATIONS

In general, the CB method requires more wavenumber samples to converge and is slower for a given N, than the other methods. This is unfortunate, since it performs well over a broader range of slope and frequency parameters.

Figure 8 shows the computation time for each of the methods on the CONVEX C1 supercomputer using single precision arithmetic. For $N > 40$ the CPU time required for CB is approximately an order of magnitude greater than for AL or WF.

Each algorithm consists of two labor intensive parts, creating the N X N matrix and solving the system. The AL, WR, and WF algorithms each require the execution of three nested loops to create the matrix. Two of these loops can be vectorized by the CONVEX fortran compiler. The additional time required for CB is due to an additional loop implied by equation 22 as compared to equation 5 for AL and equations 15 and 17 for WR and WF. For each of the methods, the LINPACK Gaussian elimination routine CGECO, optimized for the CONVEX, is used to solve the system. A conjugate gradient linear equation solver was tried, but proved to be slower than CGECO.

In Figure 8 we see the dramatic improvement in speed obtained by using an FFT in conjunction with the Waterman Fourier method.

SUMMARY

We have presented evidence that the AL, WR, WF, and CB methods are useable for slopes greater than the theoretical limit established by Millar for the Rayleigh ansatz. For a limited class of problems, (SH waves normally incident on a sinusoidal free surface), we have determined the maximum slope and frequency that each method can handle. This has been accomplished by mapping the region in slope/frequency space where the various methods converge and satisfy the energy conservation requirement. The fact that the resulting wavefields are consistent between methods indicates that the convergent solutions are indeed valid.

Of the four methods studied, it is clear that CB is the most stable and converges over the broadest range of slopes and frequencies. The AL and WF methods have convergence properties very similar to one another supporting the conclusion of Wirgin (1980) that neither is superior for steep slopes. We see that for steep slopes , AL gives erroneous results for displacement on the interface but gives valid displacements (consistent with WF and CB) beyond the topography. WR is the least stable of the four methods and converges only for low slopes.

AL possesses a potential advantage over WF for multi-layer problems if an interface is within the topography of an adjacent interface. This advantage exists only for low slopes where the Rayleigh expansion is valid both inside and outside the bounding plane of the topography, i.e. for $h/L < 0.072$. The Waterman methods do not yield solutions to the wavefield inside the topography.

We have introduced a normalization technique that improves the stability of WR and WF. This modification allows more wavenumber samples to be used in the calculations, but it does not significantly extend the slope/frequency limits of those methods.

In terms of execution time, the AL and WF methods are fastest. Using an FFT to calculate each row of the matrix in WF is faster than computing N individual integrals or Bessel functions. For nonsinusoidal interfaces the improvement in speed will be most dramatic.

The CB method, while it is the most stable, is also the slowest. It has an additional loop in the calculation of the matrix elements and requires more wavenumber samples to achieve convergence.

ACKNOWLEDGEMENT

We would like to thank Robert Parker for the use of his program PLOTXY. This research was supported by contract F19628-87-K-0029 of the Advanced Research Projects Agency of the Department of Defense and monitored by the Air Force Geophysics Laboratory. Contribution number 647 from the Program in Geosciences of the University of Texas at Dallas.

FIGURE 1 Schematic of the numerical experiments. U_I and U_R are the incident and reflected wavefields. Below the interface the shear modulus and density are μ and ρ respectively.

FIGURE 2 The "Rayleigh *ansatz*" expands the reflected wavefield below the interface as the sum of downgoing plane waves. Lippmann pointed out that the *ansatz* was incapable of representing upgoing reflected energy in the region between the interface and the plane that bounds the topography.

FIGURE 3 Energy conservation as a function of frequency and number of coefficients. Asterices represent reflected energy flux within 1% of incident flux. Plus signs represent 1-5% error. Each symbol corresponds to a separate numerical experiment. Each frame corresponds to a particular technique and slope.

FIGURE 4 Improvement in convergence due to normalization.

FIGURE 5 Displacement on the interface. Each frame corresponds to a separate numerical experiment. The AL method gives anomalous results despite satisfying energy conservation.

FIGURE 6 Dispacement on the lower plane bounding the topography (z=h), using the same experimental parameters as in Figure 5. The AL method agrees with WF and CB.

FIGURE 7 Wavenumber spectrum of reflected energy at z=h, using the same experimental parameters as in Figures 4 & 5.

FIGURE 8 Computation time on the Convex C1 supercomputer as a function of N, the number of coefficients.

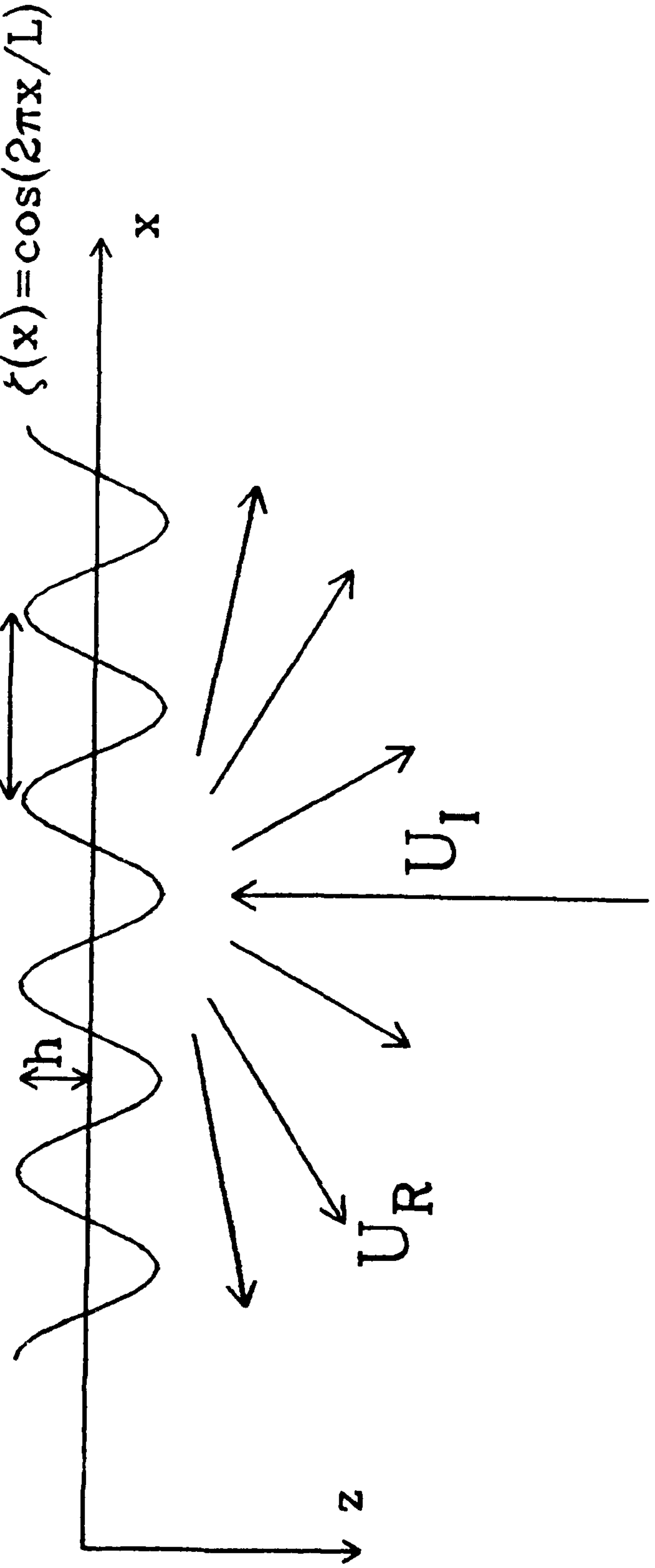

Figure 1

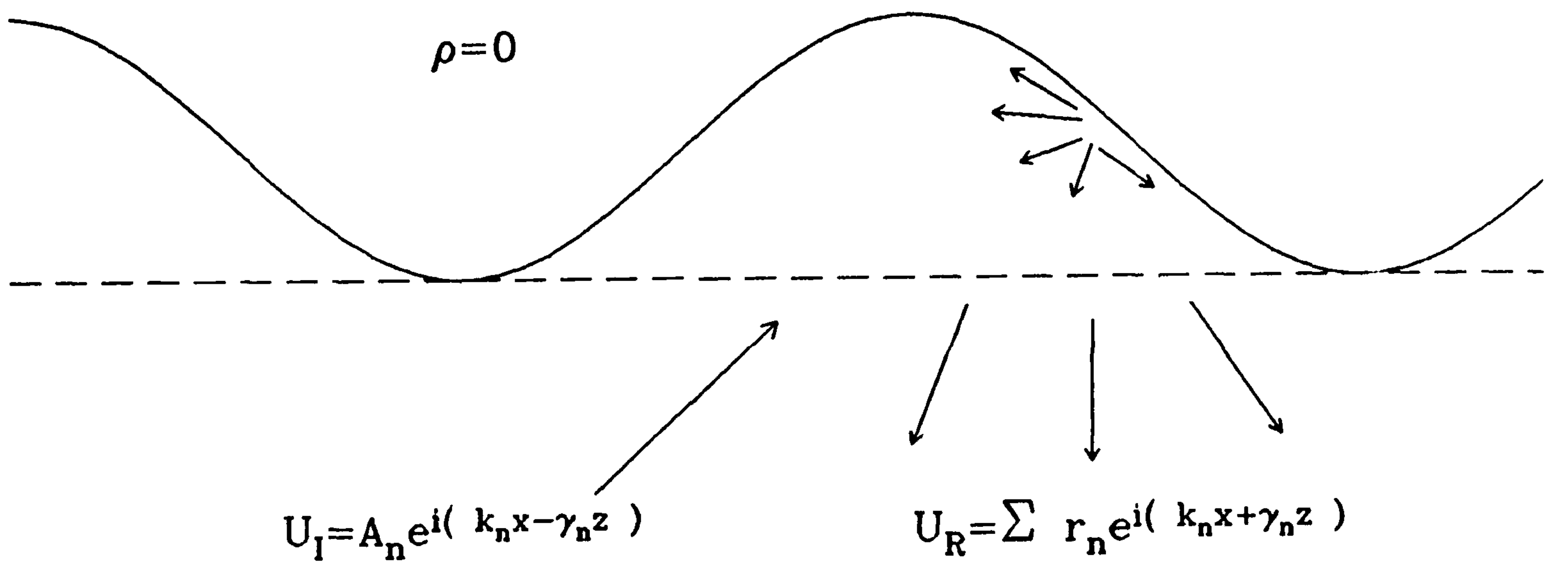

Figure 2

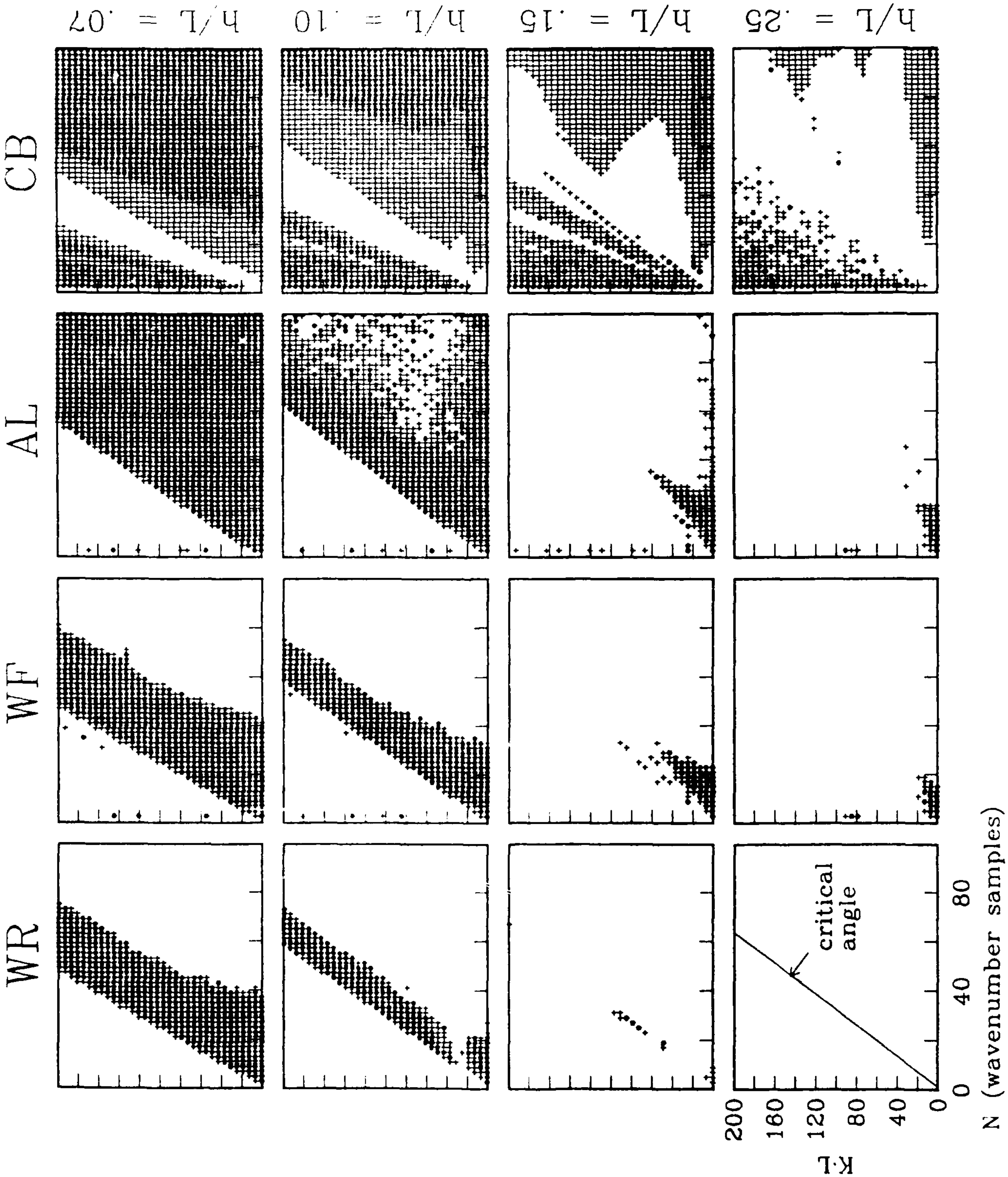
WR
WF
AL
CB
h/L = .07
h/L = .10
h/L = .15
h/L = .25
K·L
200
160
120
80
40
0
0
40
80
N (wavenumber samples)
critical angle

Figure 3

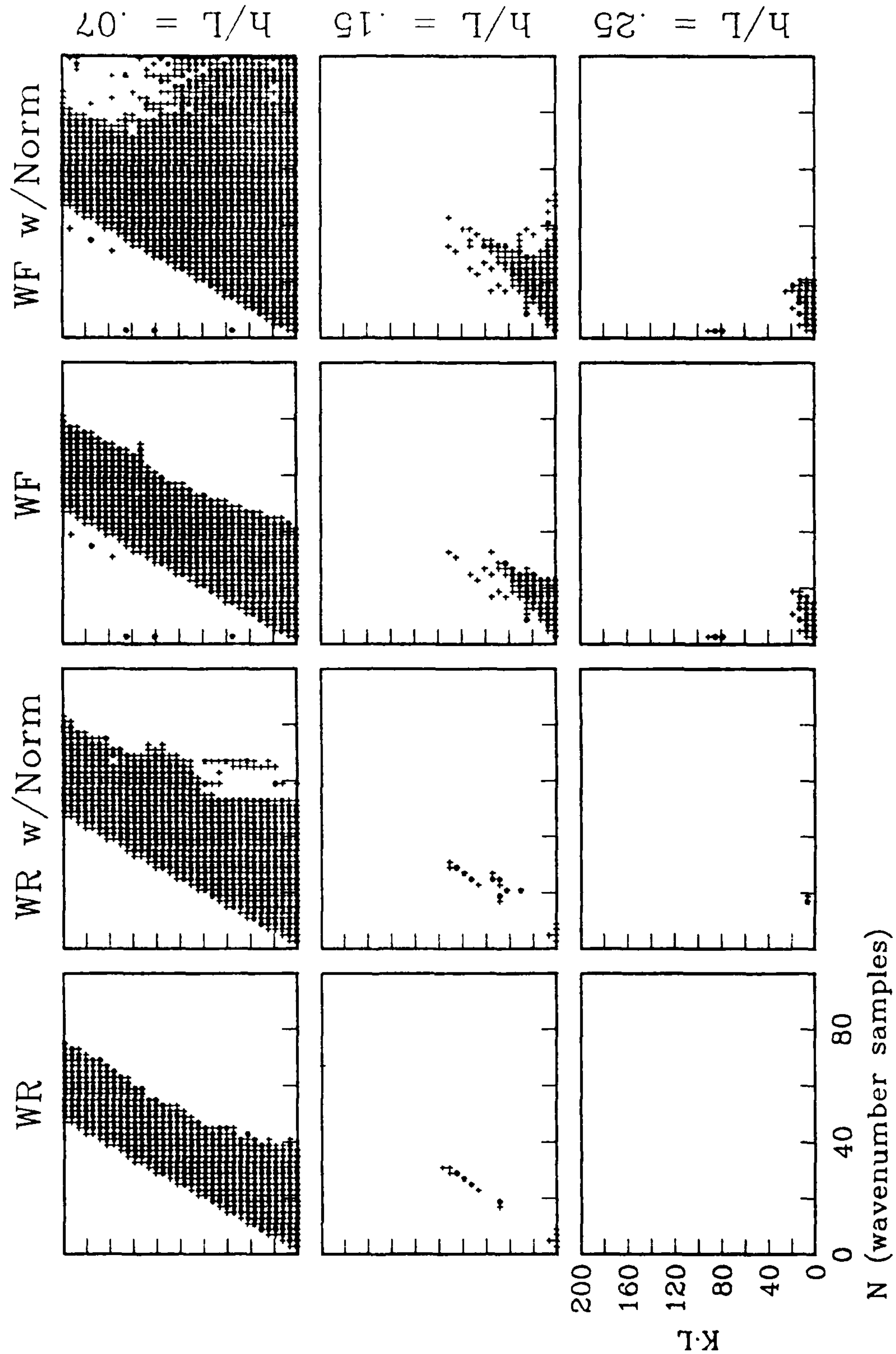
WR
WR w/Norm
WF
WF w/Norm
h/L = .07
h/L = .15
h/L = .25
K·L
200
160
120
80
40
0
0
40
80
N (wavenumber samples)

Figure 4

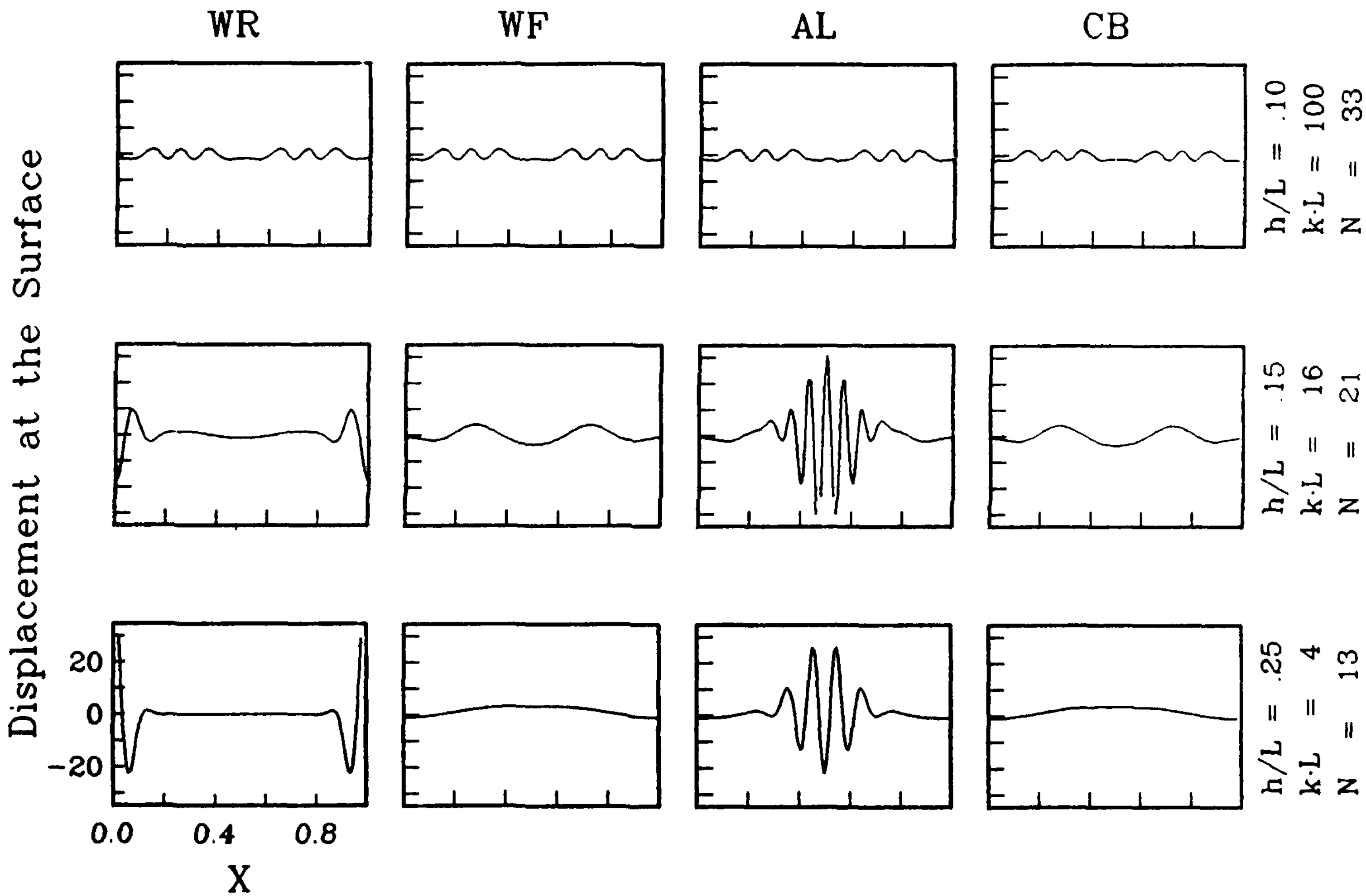
WR
WF
AL
CB
Displacement at the Surface
20
0
−20
0.0
0.4
0.8
X
h/L = .10
k·L = 100
N = 33
h/L = .15
k·L = 16
N = 21
h/L = .25
k·L = 4
N = 13

Figure 5

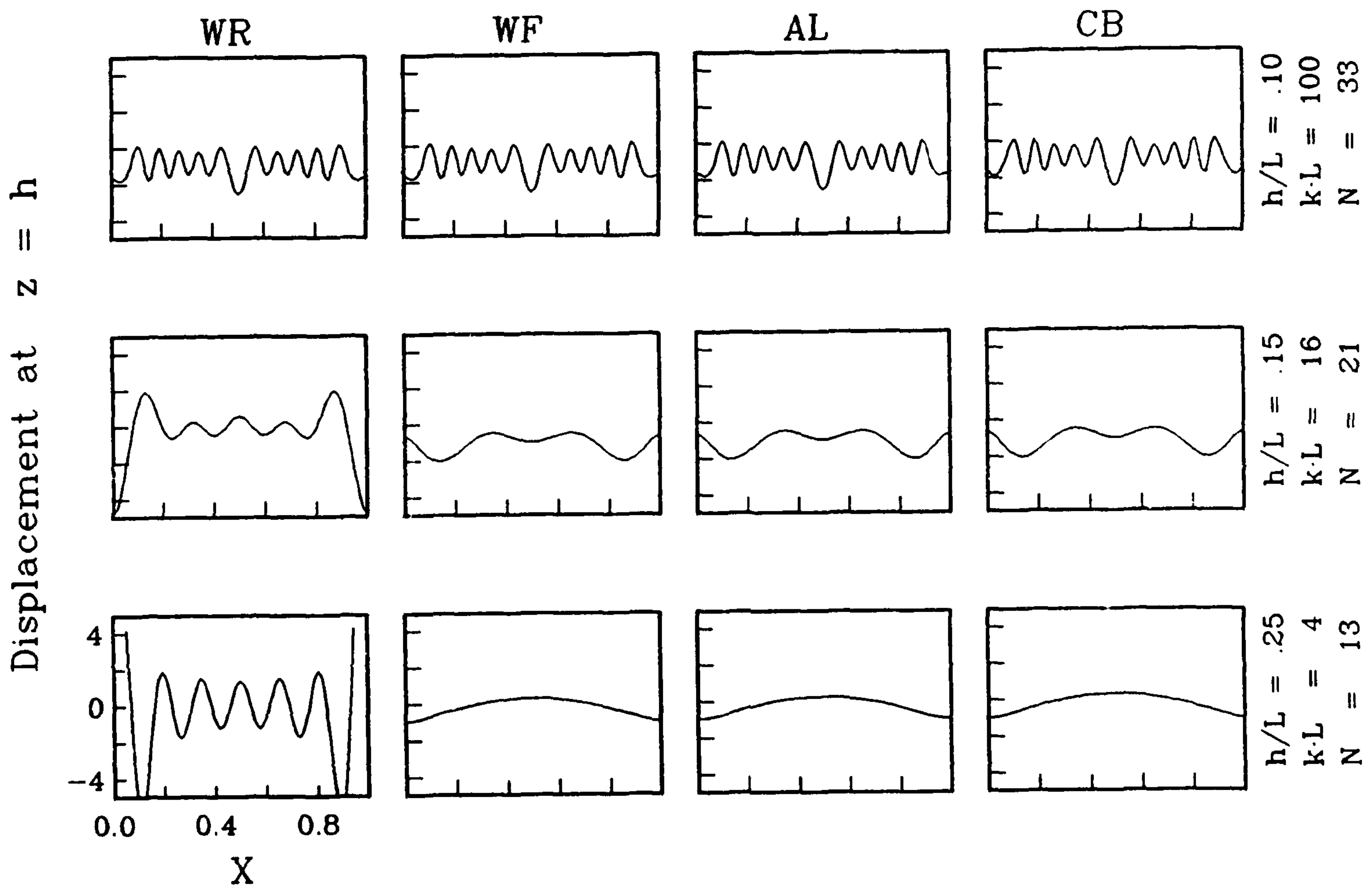
WR
WF
AL
CB
Displacement at z = h
h/L = .10
k·L = 100
N = 33
h/L = .15
k·L = 16
N = 21
h/L = .25
k·L = 4
N = 13
4
0
−4
0.0
0.4
0.8
X

Figure 6

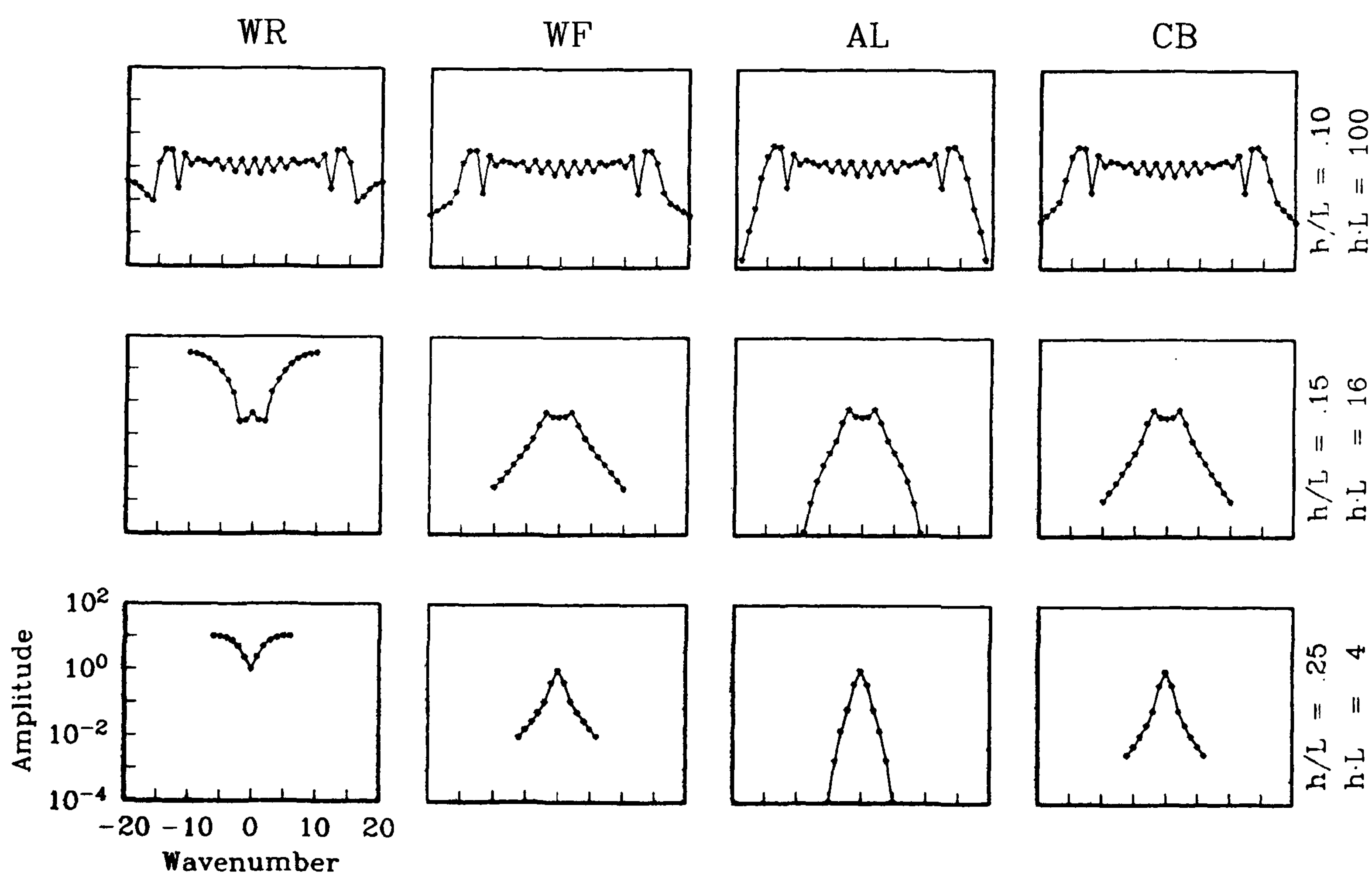

WR
WF
AL
CB
h/L = .10
h·L = 100
h/L = .15
h·L = 16
h/L = .25
h·L = 4
Amplitude
10^2
10^0
10^{-2}
10^{-4}
−20 −10 0 10 20
Wavenumber

Figure 7

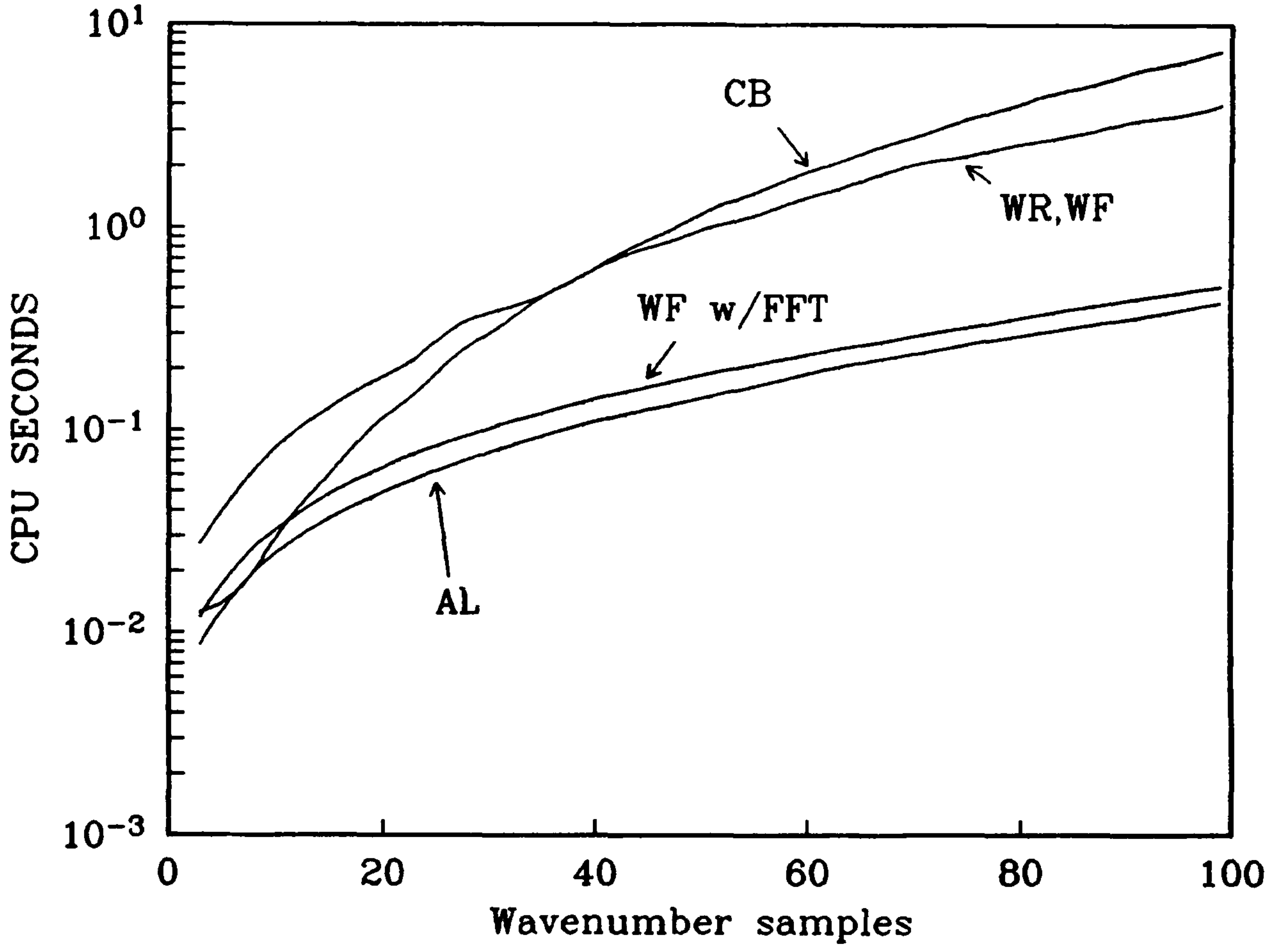

CPU SECONDS
Wavenumber samples
CB
WR,WF
WF w/FFT
AL
10^{1}
10^{0}
10^{-1}
10^{-2}
10^{-3}
0
20
40
60
80
100

Figure 8

APPENDIX I

To invoke the normalization multiply equations 12 and 13 as follow:

$$\mathbf{W}\,\mathbf{r} = \mathbf{W}\,\mathbf{Q}^{+}\,\boldsymbol{\alpha}$$

$$[\mathbf{W}]^{-1}\,\mathbf{b} = [\mathbf{W}]^{-1}\,\mathbf{Q}^{-}\,\boldsymbol{\alpha}$$

where

$$W_{mn} = \left.\begin{cases} e^{-i\gamma_n h} & n = m \\ 0 & n \neq m \end{cases}\right.$$

Then solve the new system, which has improved stability:

$$\mathbf{r}' = \mathbf{Q}^{+\prime}\,\boldsymbol{\alpha}$$

$$\mathbf{b}' = \mathbf{Q}^{-\prime}\,\boldsymbol{\alpha}$$

$$\mathbf{r}' = \mathbf{Q}^{+\prime}[\mathbf{Q}^{-\prime}]^{-1}\,\mathbf{b}'$$

Converting to the original basis functions,

$$\mathbf{r} = \mathbf{W}\,\mathbf{Q}^{+\prime}\,[\mathbf{Q}^{-\prime}]^{-1}\,\mathbf{W}\,\mathbf{a}.$$

REFERENCES

Aki, K. and K. L. Larner (1970). Surface motion of a layered medium having an irregular interface due to incident plane SH waves, *J. Geophys. Res.* **75**, 933-954.

Campillo, M. and M. Bouchon (1985). Synthetic SH seismograms in a laterally varying medium by the discrete wavenumber method, *Geophys. J. R. Astr. Soc.* **83**, 307-317.

Jiracek, G. R. (1973) Numerical comparison of a modified Rayleigh approach with other rough surface EM scattering solutions, *IEEE Trans. Antenna Propagation* **AP-21**, 393-396.

Lakhtakia, A., V. K. Varadan, and V. V. Varadan (1985a). Scattering by a partially illuminated, doubly infinite surface, *J. Acoust. Soc. Am.* **77**, 1999-2004.

Lakhtakia, A., V. K. Varadan, and V. V. Varadan (1985b). On the acoustic response of a deeply corrugated periodic surface - a hybrid T-matrix approach, *J. Acoust. Soc. Am.* **78**, 2100-2104.

Lakhtakia, A., V. K. Varadan, and V. V. Varadan (1986). Reply to "Comments on 'On the acoustic response of a deeply corrugated periodic surface - a hybrid T-matrix approach'", *J. Acoust. Soc. Am.* **80**, 964-965.

Larner, K. L. (1970) Near-receiver scattering of teleseismic body waves in layered crust-mantle models having irregular interfaces, *Ph.D. thesis*, Massachusetts institute of Technology, Cambridge, Massachusetts.

Lippmann B. A. (1953). Note on the theory of gratings, *J. Opt. Soc. Amer.* **43**, 408.

Masel, R. I., R. P. Merrill, and W. H. Miller (1975). Quantum scattering from a sinusoidal hard wall: Atomic diffraction from solid surfaces, *Phys. Rev. B* **12**, 5545-5551.

Millar, R. F. (1971). On the Rayleigh assumption in scattering by a periodic surface, *Proc. Camb. Philos. Soc.* **69**, 217-255.

Petit R. and M. Cadilhac (1966). Sur la diffraction d'une onde plane par un réseau infinitement conducteur, *C. R. Acad. Sci., Ser. B.* **262**, 468-471.

Rayleigh, Lord (J. W. Strutt) (1907). On the dynamical theory of gratings, *Proc. Roy. Soc., Ser. A.* **79**, 399-416.

Varadan, V. K., A. Lakhtakia, V. V. Varadan, and C. A. Langston (1987). Radiation characteristics of elastodynamic line sources buried in layered media with periodic interfaces. I. SH-wave analysis, *Bull. Seism. Soc. Am.* **77**, 2181-2191.

Waterman, P. C. (1975). Scattering by periodic surfaces, *J. Acoust. Soc. Am.* **57**, 791-802.

Wirgin, A. (1980). Reflection from a corrugated surface, J. Acoust. Soc. Am. **68**, 692-699.

Wirgin, A. (1986). Comments on "On the acoustic response of a deeply corrugated periodic surface - a hybrid T-matrix approach", *J. Acoust. Soc. Am.* **80**, 963-965.

Prof. Thomas Ahrens
Seismological Lab, 252-21
Division of Geological & Planetary Sciences
California Institute of Technology
Pasadena, CA 91125

Prof. Charles B. Archambeau
CIRES
University of Colorado
Boulder, CO 80309

Prof. Muawia Barazangi
Institute for the Study of the Continent
Cornell University
Ithaca, NY 14853

Dr. Douglas R. Baumgardt
ENSCO, Inc
5400 Port Royal Road
Springfield, VA 22151-2388

Prof. Jonathan Berger
IGPP, A-025
Scripps Institution of Oceanography
University of California, San Diego
La Jolla, CA 92093

Dr. Lawrence J. Burdick
Woodward-Clyde Consultants
566 El Dorado Street
Pasadena, CA 91109-3245

Dr. Karl Coyner
New England Research, Inc.
76 Olcott Drive
White River Junction, VT 05001

Prof. Vernon F. Cormier
Department of Geology & Geophysics
U-45, Room 207
The University of Connecticut
Storrs, CT 06268

Prof. Steven Day
Department of Geological Sciences
San Diego State University
San Diego, CA 92182

Dr. Zoltan A. Der
ENSCO, Inc.
5400 Port Royal Road
Springfield, VA 22151-2388

Prof. John Ferguson
Center for Lithospheric Studies
The University of Texas at Dallas
P.O. Box 830688
Richardson, TX 75083-0688

Prof. Stanley Flatte
Applied Sciences Building
University of California
Santa Cruz, CA 95064

Dr. Alexander Florence
SRI International
333 Ravenswood Avenue
Menlo Park, CA 94025-3493

Prof. Henry L. Gray
Vice Provost and Dean
Department of Statistical Sciences
Southern Methodist University
Dallas, TX 75275

Dr. Indra Gupta
Teledyne Geotech
314 Montgomery Street
Alexandria, VA 22314

Prof. David G. Harkrider
Seismological Laboratory
Division of Geological & Planetary Sciences
California Institute of Technology
Pasadena, CA 91125

Prof. Donald V. Helmberger
Seismological Laboratory
Division of Geological & Planetary Sciences
California Institute of Technology
Pasadena, CA 91125

Prof. Eugene Herrin
Institute for the Study of Earth and Man
GeophysicalLaboratory
Southern Methodist University
Dallas, TX 75275

Prof . Robert B. Herrmann
Department of Earth & Atmospheric Sciences
St. Louis University
St. Louis, MO 63156

Prof. Bryan Isacks
Cornell University
Department of Geological Sciences
SNEE Hall
Ithaca, NY 14850

Dr. Rong-Song Jih
Teledyne Geotech
314 Montgomery Street
Alexandria, VA 22314

Prof. Lane R. Johnson
Seismographic Station
University of California
Berkeley, CA 94720

Prof. Alan Kafka
Department of Geology & Geophysics
Boston College
Chestnut Hill, MA 02167

Prof. Fred K. Lamb
University of Illinois at Urbana-Champaign
Department of Physics
1110 West Green Street
Urbana, IL 61801

Prof. Charles A. Langston
Geosciences Department
403 Deike Building
The Pennsylvania State University
University Park, PA 16802

Prof. Thorne Lay
Department of Geological Sciences
1006 C.C. Little Building
University of Michigan
Ann Arbor, MI 48109-1063

Prof. Arthur Lerner-Lam
Lamont-Doherty Geological Observatory
of Columbia University
Palisades, NY 10964

Dr. Christopher Lynnes
Teledyne Geotech
314 Montgomery Street
Alexandria, VA 22314

Prof. Peter Malin
University of California at Santa Barbara
Institute for Crustal Studies
Santa Barbara, CA 93106

Dr. Randolph Martin, III
New England Research, Inc.
76 Olcott Drive
White River Junction, VT 05001

Dr. Gary McCartor
Mission Research Corporation
735 State Street
P.O. Drawer 719
Santa Barbara, CA 93102 (2 copies)

Prof. Thomas V. McEvilly
Seismographic Station
University of California
Berkeley, CA 94720

Dr. Keith L. McLaughlin
S-CUBED
A Division of Maxwell Laboratory
P.O. Box 1620
La Jolla, CA 92038-1620

Prof. William Menke
Lamont-Doherty Geological Observatory
of Columbia University
Palisades, NY 10964

Stephen Miller
SRI International
333 Ravenswood Avenue
Box AF 116
Menlo Park, CA 94025-3493

Prof. Bernard Minster
IGPP, A-025
Scripps Institute of Oceanography
University of California, San Diego
La Jolla, CA 92093

Prof. Brian J. Mitchell
Department of Earth & Atmospheric Sciences
St. Louis University
St. Louis, MO 63156

Mr. Jack Murphy
S-CUBED, A Division of Maxwell Laboratory
11800 Sunrise Valley Drive
Suite 1212
Reston, VA 22091 (2 copies)

Dr. Bao Nguyen
GL/LWH
Hanscom AFB, MA 01731-5000

Prof. John A. Orcutt
IGPP, A-025
Scripps Institute of Oceanography
University of California, San Diego
La Jolla, CA 92093

Prof. Keith Priestley
University of Nevada
Mackay School of Mines
Reno, NV 89557

Prof. Paul G. Richards
Lamont-Doherty Geological Observatory
of Columbia University
Palisades, NY 10964

Dr. Wilmer Rivers
Teledyne Geotech
314 Montgomery Street
Alexandria, VA 22314

Dr. Alan S. Ryall, Jr.
Center for Seismic Studies
1300 North 17th Street
Suite 1450
Arlington, VA 22209-2308

Prof. Charles G. Sammis
Center for Earth Sciences
University of Southern California
University Park
Los Angeles, CA 90089-0741

Prof. Christopher H. Scholz
Lamont-Doherty Geological Observatory
of Columbia University
Palisades, NY 10964

Prof. David G. Simpson
Lamont-Doherty Geological Observatory
of Columbia University
Palisades, NY 10964

Dr. Jeffrey Stevens
S-CUBED
A Division of Maxwell Laboratory
P.O. Box 1620
La Jolla, CA 92038-1620

Prof. Brian Stump
Institute for the Study of Earth & Man
Geophysical Laboratory
Southern Methodist University
Dallas, TX 75275

Prof. Jeremiah Sullivan
University of Illinois at Urbana-Champaign
Department of Physics
1110 West Green Street
Urbana, IL 61801

Prof. Clifford Thurber
University of Wisconsin-Madison
Department of Geology & Geophysics
1215 West Dayton Street
Madison, WS 53706

Prof. M. Nafi Toksoz
Earth Resources Lab
Massachusetts Institute of Technology
42 Carleton Street
Cambridge, MA 02142

Prof. John E. Vidale
University of California at Santa Cruz
Seismological Laboratory
Santa Cruz, CA 95064

Prof. Terry C. Wallace
Department of Geosciences
Building #77
University of Arizona
Tucson, AZ 85721

Dr. Raymond Willeman
GL/LWH
Hanscom AFB, MA 01731-5000

Dr. Lorraine Wolf
GL/LWH
Hanscom AFB, MA 01731-5000

Prof. Francis T. Wu
Department of Geological Sciences
State University of New York
at Binghamton
Vestal, NY 13901

Dr. Monem Abdel-Gawad
Rockwell International Science Center
1049 Camino Dos Rios
Thousand Oaks, CA 91360

Prof. Keiiti Aki
Center for Earth Sciences
University of Southern California
University Park
Los Angeles, CA 90089-0741

Prof. Shelton S. Alexander
Geosciences Department
403 Deike Building
The Pennsylvania State University
University Park, PA 16802

Dr. Ralph Archuleta
Department of Geological Sciences
University of California at Santa Barbara
Santa Barbara, CA 93102

Dr. Thomas C. Bache, Jr.
Science Applications Int'l Corp.
10210 Campus Point Drive
San Diego, CA 92121 (2 copies)

J. Barker
Department of Geological Sciences
State University of New York
at Binghamton
Vestal, NY 13901

Dr. T.J. Bennett
S-CUBED
A Division of Maxwell Laboratory
11800 Sunrise Valley Drive, Suite 1212
Reston, VA 22091

Mr. William J. Best
907 Westwood Drive
Vienna, VA 22180

Dr. N. Biswas
Geophysical Institute
University of Alaska
Fairbanks, AK 99701

Dr. G.A. Bollinger
Department of Geological Sciences
Virginia Polytechnical Institute
21044 Derring Hall
Blacksburg, VA 24061

Dr. Stephen Bratt
Science Applications Int'l Corp.
10210 Campus Point Drive
San Diego, CA 92121

Michael Browne
Teledyne Geotech
3401 Shiloh Road
Garland, TX 75041

Mr. Roy Burger
1221 Serry Road
Schenectady, NY 12309

Dr. Robert Burridge
Schlumberger-Doll Research Center
Old Quarry Road
Ridgefield, CT 06877

Dr. Jerry Carter
Rondout Associates
P.O. Box 224
Stone Ridge, NY 12484

Dr. W. Winston Chan
Teledyne Geotech
314 Montgomery Street
Alexandria, VA 22314-1581

Dr. Theodore Cherry
Science Horizons, Inc.
710 Encinitas Blvd., Suite 200
Encinitas, CA 92024 (2 copies)

Prof. Jon F. Claerbout
Department of Geophysics
Stanford University
Stanford, CA 94305

Prof. Robert W. Clayton
Seismological Laboratory
Division of Geological & Planetary Sciences
California Institute of Technology
Pasadena, CA 91125

Prof. F. A. Dahlen
Geological and Geophysical Sciences
Princeton University
Princeton, NJ 08544-0636

Prof. Anton W. Dainty
Earth Resources Lab
Massachusetts Institute of Technology
42 Carleton Street
Cambridge, MA 02142

Prof. Stephen Grand
University of Texas at Austin
Department of Geological Sciences
Austin, TX 78713-7909

Prof. Adam Dziewonski
Hoffman Laboratory
Harvard University
20 Oxford St
Cambridge, MA 02138

Prof. Roy Greenfield
Geosciences Department
403 Deike Building
The Pennsylvania State University
University Park, PA 16802

Prof. John Ebel
Department of Geology & Geophysics
Boston College
Chestnut Hill, MA 02167

Dan N. Hagedorn
Battelle
Pacific Northwest Laboratories
Battelle Boulevard
Richland, WA 99352

Eric Fielding
SNEE Hall
INSTOC
Cornell University
Ithaca, NY 14853

Kevin Hutchenson
Department of Earth Sciences
St. Louis University
3507 Laclede
St. Louis, MO 63103

Prof. Donald Forsyth
Department of Geological Sciences
Brown University
Providence, RI 02912

Prof. Thomas H. Jordan
Department of Earth, Atmospheric
and Planetary Sciences
Massachusetts Institute of Technology
Cambridge, MA 02139

Prof. Art Frankel
Mail Stop 922
Geological Survey
790 National Center
Reston, VA 22092

Robert C. Kemerait
ENSCO, Inc.
445 Pineda Court
Melbourne, FL 32940

Dr. Anthony Gangi
Texas A&M University
Department of Geophysics
College Station, TX 77843

William Kikendall
Teledyne Geotech
3401 Shiloh Road
Garland, TX 75041

Dr. Freeman Gilbert
Inst. of Geophysics & Planetary Physics
University of California, San Diego
P.O. Box 109
La Jolla, CA 92037

Prof. Leon Knopoff
University of California
Institute of Geophysics & Planetary Physics
Los Angeles, CA 90024

Mr. Edward Giller
Pacific Sierra Research Corp.
1401 Wilson Boulevard
Arlington, VA 22209

Prof. L. Timothy Long
School of Geophysical Sciences
Georgia Institute of Technology
Atlanta, GA 30332

Dr. Jeffrey W. Given
Sierra Geophysics
11255 Kirkland Way
Kirkland, WA 98033

Prof. Art McGarr
Mail Stop 977
Geological Survey
345 Middlefield Rd.
Menlo Park, CA 94025

Dr. George Mellman
Sierra Geophysics
11255 Kirkland Way
Kirkland, WA 98033

Prof. John Nabelek
College of Oceanography
Oregon State University
Corvallis, OR 97331

Prof. Geza Nagy
University of California, San Diego
Department of Ames, M.S. B-010
La Jolla, CA 92093

Prof. Amos Nur
Department of Geophysics
Stanford University
Stanford, CA 94305

Prof. Jack Oliver
Department of Geology
Cornell University
Ithaca, NY 14850

Prof. Robert Phinney
Geological & Geophysical Sciences
Princeton University
Princeton, NJ 08544-0636

Dr. Paul Pomeroy
Rondout Associates
P.O. Box 224
Stone Ridge, NY 12484

Dr. Jay Pulli
RADIX System, Inc.
2 Taft Court, Suite 203
Rockville, MD 20850

Dr. Norton Rimer
S-CUBED
A Division of Maxwell Laboratory
P.O. Box 1620
La Jolla, CA 92038-1620

Prof. Larry J. Ruff
Department of Geological Sciences
1006 C.C. Little Building
University of Michigan
Ann Arbor, MI 48109-1063

Dr. Richard Sailor
TASC Inc.
55 Walkers Brook Drive
Reading, MA 01867

Thomas J. Sereno, Jr.
Science Application Int'l Corp.
10210 Campus Point Drive
San Diego, CA 92121

John Sherwin
Teledyne Geotech
3401 Shiloh Road
Garland, TX 75041

Prof. Robert Smith
Department of Geophysics
University of Utah
1400 East 2nd South
Salt Lake City, UT 84112

Prof. S. W. Smith
Geophysics Program
University of Washington
Seattle, WA 98195

Dr. Stewart Smith
IRIS Inc.
1616 North Fort Myer Drive
Suite 1440
Arlington, VA 22209

Dr. George Sutton
Rondout Associates
P.O. Box 224
Stone Ridge, NY 12484

Prof. L. Sykes
Lamont-Doherty Geological Observatory
of Columbia University
Palisades, NY 10964

Prof. Pradeep Talwani
Department of Geological Sciences
University of South Carolina
Columbia, SC 29208

Prof. Ta-liang Teng
Center for Earth Sciences
University of Southern California
University Park
Los Angeles, CA 90089-0741

Dr. R.B. Tittmann
Rockwell International Science Center
1049 Camino Dos Rios
P.O. Box 1085
Thousand Oaks, CA 91360

Dr. Gregory van der Vink
IRIS, Inc.
1616 North Fort Myer Drive
Suite 1440
Arlington, VA 22209

William R. Walter
Seismological Laboratory
University of Nevada
Reno, NV 89557

Dr. Gregory Wojcik
Weidlinger Associates
4410 El Camino Real
Suite 110
Los Altos, CA 94022

Prof. John H. Woodhouse
Hoffman Laboratory
Harvard University
20 Oxford Street
Cambridge, MA 02138

Dr. Gregory B. Young
ENSCO, Inc.
5400 Port Royal Road
Springfield, VA 22151-2388

Dr. Ralph Alewine III
DARPA/NMRO
1400 Wilson Boulevard
Arlington, VA 01731-5000

Mr. James C. Battis
GL/LWH
Hanscom AFB, MA 22209-2308

Dr. Robert Blandford
DARPA/NMRO
1400 Wilson Boulevard
Arlington, VA 87185

Eric Chael
Division 9241
Sandia Laboratory
Albuquerque, NM 01731-5000

Dr. John J. Cipar
GL/LWH
Hanscom AFB, MA 01731-5000

Mr. Jeff Duncan
Office of Congressman Markey
2133 Rayburn House Bldg.
Washington, D.C. 20515

Dr. Jack Evernden
USGS - Earthquake Studies
345 Middlefield Road
Menlo Park, CA 94025

Art Frankel
USGS
922 National Center
Reston, VA 22092

Dr. T. Hanks
USGS
Nat'l Earthquake Research Center
345 Middlefield Road
Menlo Park, CA 94025

Dr. James Hannon
Lawrence Livermore Nat'l Laboratory
P.O. Box 808
Livermore, CA 94550

Paul Johnson
ESS-4, Mail Stop J979
Los Alamos National Laboratory
Los Alamos, NM 87545

Janet Johnston
GL/LWH
Hanscom AFB, MA 01731-5000

Dr. Katharine Kadinsky-Cade
GL/LWH
Hanscom AFB, MA 01731-5000

Ms. Ann Kerr
IGPP, A-025
Scripps Institute of Oceanography
University of California, San Diego
La Jolla, CA 92093

Dr. Max Koontz
US Dept of Energy/DP 5
Forrestal Building
1000 Independence Avenue
Washington, DC 20585

Dr. W.H.K. Lee
Office of Earthquakes, Volcanoes,
& Engineering
345 Middlefield Road
Menlo Park, CA 94025

Dr. William Leith
U.S. Geological Survey
Mail Stop 928
Reston, VA 22092

Dr. Richard Lewis
Director, Earthquake Engineering & Geophysics
U.S. Army Corps of Engineers
Box 631
Vicksburg, MS 39180

James F. Lewkowicz
GL/LWH
Hanscom AFB, MA 01731-5000

Mr. Alfred Lieberman
ACDA/VI-OA'State Department Bldg
Room 5726
320 - 21st Street, NW
Washington, DC 20451

Stephen Mangino
GL/LWH
Hanscom AFB, MA 01731-5000

Dr. Robert Masse
Box 25046, Mail Stop 967
Denver Federal Center
Denver, CO 80225

Art McGarr
U.S. Geological Survey, MS-977
345 Middlefield Road
Menlo Park, CA 94025

Richard Morrow
ACDA/VI, Room 5741
320 21st Street N.W
Washington, DC 20451

Dr. Keith K. Nakanishi
Lawrence Livermore National Laboratory
P.O. Box 808, L-205
Livermore, CA 94550

Dr. Carl Newton
Los Alamos National Laboratory
P.O. Box 1663
Mail Stop C335, Group ESS-3
Los Alamos, NM 87545

Dr. Kenneth H. Olsen
Los Alamos Scientific Laboratory
P.O. Box 1663
Mail Stop C335, Group ESS-3
Los Alamos, NM 87545

Howard J. Patton
Lawrence Livermore National Laboratory
P.O. Box 808, L-205
Livermore, CA 94550

Mr. Chris Paine
Office of Senator Kennedy, SR 315

United States Senate
Washington, DC 20510

Colonel Jerry J. Perrizo
AFOSR/NP, Building 410
Bolling AFB
Washington, DC 20332-6448

Dr. Frank F. Pilotte
HQ AFTAC/TT
Patrick AFB, FL 32925-6001

Katie Poley
CIA-OSWR/NED
Washington, DC 20505

Mr. Jack Rachlin
U.S. Geological Survey
Geology, Rm 3 C136
Mail Stop 928 National Center
Reston, VA 22092

Dr. Robert Reinke
WL/NTESG
Kirtland AFB, NM 87117-6008

Dr. Byron Ristvet
HQ DNA, Nevada Operations Office
Attn: NVCG
P.O. Box 98539
Las Vegas, NV 89193

Dr. George Rothe
HQ AFTAC/TGR
Patrick AFB, FL 32925-6001

Dr. Michael Shore
Defense Nuclear Agency/SPSS
6801 Telegraph Road
Alexandria, VA 22310

Donald L. Springer
Lawrence Livermore National Laboratory
P.O. Box 808, L-205
Livermore, CA 94550

Dr. Lawrence Turnbull
OSWR/NED
Central Intelligence Agency, Room 5G48
Washington, DC 20505

Dr. Thomas Weaver
Los Alamos National Laboratory
P.O. Box 1663, Mail Stop C335
Los Alamos, NM 87545

J.J. Zucca
Lawrence Livermore National Laboratory
Box 808
Livermore, CA 94550

GL/SULL
Research Library
Hanscom AFB , MA 01731-5000 (2 copies)

Secretary of the Air Force (SAFRD)

Washington, DC 20330

Office of the Secretary Defense
DDR & E
Washington, DC 20330

HQ DNA
Attn: Technical Library
Washington, DC 20305

DARPA/RMO/RETRIEVAL
1400 Wilson Boulevard
Arlington, VA 22209

DARPA/RMO/Security Office
1400 Wilson Boulevard
Arlington, VA 22209

Geophysics Laboratory
Attn: XO
Hanscom AFB, MA 01731-5000

Geophysics Laboratory
Attn: LW
Hanscom AFB, MA 01731-5000

DARPA/PM
1400 Wilson Boulevard
Arlington, VA 22209

Defense Technical Information Center
Cameron Station
Alexandria, VA 22314 (5 copies)

Defense Intelligence Agency
Directorate for Scientific &
Technical Intelligence
Washington, DC 20301

AFTAC/CA
(STINFO)
Patrick AFB, FL 32925-6001

TACTEC
Battelle Memorial Institute
505 King Avenue
Columbus, OH 43201 (Final Report Only)

Mr. Charles L. Taylor
GL/LWH

Hanscom AFB, MA 01731-5000

Dr. Ramon Cabre, S.J.
Observatorio San Calixto
Casilla 5939
La Paz, Bolivia

Prof. Hans-Peter Harjes
Institute for Geophysik
Ruhr University/Bochum
P.O. Box 102148
4630 Bochum 1, FRG

Prof. Eystein Husebye
NTNF/NORSAR
P.O. Box 51
N-2007 Kjeller, NORWAY

Prof. Brian L.N. Kennett
Research School of Earth Sciences
Institute of Advanced Studies
G.P.O. Box 4
Canberra 2601, AUSTRALIA

Dr. Bernard Massinon
Societe Radiomana
27 rue Claude Bernard
75005 Paris, FRANCE (2 Copies)

Dr. Pierre Mecheler
Societe Radiomana
27 rue Claude Bernard
75005 Paris, FRANCE

Dr. Svein Mykkeltveit
NTNF/NORSAR
P.O. Box 51
N-2007 Kjeller, NORWAY

Dr. Peter Basham
Earth Physics Branch
Geological Survey of Canada
1 Observatory Crescent
Ottawa, Ontario, CANADA K1A 0Y3

Dr. Eduard Berg
Institute of Geophysics
University of Hawaii
Honolulu, HI 96822

Dr. Michel Bouchon
I.R.I.G.M.-B.P. 68
38402 St. Martin D'Heres
Cedex, FRANCE

Dr. Hilmar Bungum
NTNF/NORSAR
P.O. Box 51
N-2007 Kjeller, NORWAY

Dr. Michel Campillo
Observatoire de Grenoble
I.R.I.G.M.-B.P. 53
38041 Grenoble, FRANCE

Dr. Kin Yip Chun
Geophysics Division
Physics Department
University of Toronto
Ontario, CANADA M5S 1A7

Dr. Alan Douglas
Ministry of Defense
Blacknest, Brimpton
Reading RG7-4RS, UNITED KINGDOM

Dr. Roger Hansen
NTNF/NORSAR
P.O. Box 51
N-2007 Kjeller, NORWAY

Dr. Manfred Henger
Federal Institute for Geosciences & Nat'l Res.
Postfach 510153
D-3000 Hanover 51, FRG

Ms. Eva Johannisson
Senior Research Officer
National Defense Research Inst.
P.O. Box 27322
S-102 54 Stockholm, SWEDEN

Dr. Fekadu Kebede
Seismological Section
Box 12019
S-750 Uppsala, SWEDEN

Dr. Tormod Kvaerna
NTNF/NORSAR
P.O. Box 51
N-2007 Kjeller, NORWAY

Dr. Peter Marshal
Procurement Executive
Ministry of Defense
Blacknest, Brimpton
Reading FG7-4RS, UNITED KINGDOM

Prof. Ari Ben-Menahem
Department of Applied Mathematics
Weizman Institute of Science
Rehovot, ISRAEL 951729

Dr. Robert North
Geophysics Division
Geological Survey of Canada
1 Observatory Crescent
Ottawa, Ontario, CANADA K1A 0Y3

Dr. Frode Ringdal
NTNF/NORSAR
P.O. Box 51
N-2007 Kjeller, NORWAY

Dr. Jorg Schlittenhardt
Federal Institute for Geosciences & Nat'l Res.
Postfach 510153
D-3000 Hannover 51, FEDERAL REPUBLIC OF GERMANY

Prof. Daniel Walker
University of Hawaii
Institute of Geophysics
Honolulu, HI 96822